High-resolution four-wave-mixing spectroscopy of collision-induced narrow resonances in Doppler-broadened systems

Jing Liu and D. G. Steel
Department of Physics and Department of Electrical Engineering, University of Michigan, The Harrison M. Randall Laboratory of Physics, Ann Arbor, Michigan 48109-1120
(Received 8 April 1988)

We report a series of measurements of the nearly degenerate four-wave-mixing response in atomic sodium in the presence of a helium buffer gas. The results show the line shape associated with both the ground-state and excited-state dynamics. The line shape evolves as a function of pressure from a dip at a pressure of 0 Torr to a spike at a few Torr due to the presence of collisions. The width of the spike is determined by residual Doppler broadening. At higher pressure ($\geq$ 10 Torr), the width of the spike is further narrowed below the residual Doppler width. The additional reduction is due to a form of Dicke narrowing associated with the dynamics of the lower- and upper-level excitations. The results are in qualitative agreement with a perturbation solution of the density-matrix equations which include the effects of velocity-changing collisions and state-changing collisions.

I. INTRODUCTION

The effects of state coupling to an external reservoir have given rise to a number of interesting phenomena in four-wave-mixing (FWM) laser spectroscopy. For example, in homogeneously broadened material (such as an atomic system with the laser detuning large compared with the Doppler width), pressure-induced extra resonances in FWM (PIER-4) were first predicted[1] and observed[2] by Bloembergen and coworkers and further described in a dressed-atom calculation.[3] Extra resonances have also been predicted in the presence of strong optical fields[4,5] and as a result of correlated fluctuations in the fields.[6] The general field of dephasing-induced phenomena is the subject of a recent review.[7] In Doppler-broadened material, state specific coupling due to collisions was reported[8,9] and was shown to be the origin of narrow resonances in nearly degenerate FWM (NDFWM).[10] Narrow resonances have also been observed in *collisionless* Doppler-broadened systems and are the result of nonconservation of population,[11] alignment, or orientation[12] due to radiative decay. (In this problem, the reservoir is the vacuum radiation field which gives rise to spontaneous emission.)

In collision-induced narrow resonances in Doppler-broadened systems, collisions have two major effects: state-changing collisions cause transitions between different states (including magnetic substates) and result in decay of population, alignment and orientation; velocity-changing collisions induce decay of the resonant-selected-velocity subgroup to other velocity subgroups within the same energy state. Equally important, however, is that velocity-changing collisions can also result in nonresonant atoms being scattered into resonance.

The effects of these collisions on the FWM response is seen on the FWM resonance associated with dynamics of the upper and lower levels, as discussed in detail below. This resonance is actually the sum of two resonances with widths determined by the upper-state and lower-state decay rate, respectively. In a closed, simple, two-level system (i.e., no degeneracies), defined as one which conserves population (to within an overall decay constant), the dynamics of the upper and lower levels are associated with populations. The amplitude of the resonance associated with the lower level is zero and is not observed. If the system is open, for example, due to state-changing collisions which cause decay of the excited state to some nearby state, then the resonance associated with the lower-state width can be observed. This resonance is often quite pronounced because the lower-state dynamics are often slower than those of the upper state, resulting in a very narrow resonance with a width less than the excited-state emission rate.

The situation is slightly more complex in a Doppler-broadened system, but the narrow resonance effect can still be observed in the presence of collisions even if the total population remains conserved (i.e., even if the system is closed). In a Doppler-broadened system interacting with a narrow-band laser, only the resonant-selected-velocity subgroup contributes to the FWM signal. However, velocity-changing collisions result in atoms in the velocity-selected subgroup undergoing decay to other velocity groups. Hence, even though population is conserved over the entire velocity distribution, it is not conserved within the specific subgroup. Specifically, if the upper- and lower-level velocity-changing collision rates are different, then the resonant subgroup appears open and the resonance associated with lower-level dynamics is observed.

The purpose of this paper is to report on high-resolution spectroscopy measurements of collision-induced narrow resonances using backward nearly degenerate four-wave mixing (NDFWM). In this work the contribution of the residual Doppler width has been minimized. We are thus able to resolve the substructure of the line shape and determine a detailed picture of the complex evolution of the NDFWM line shape as a function of buffer gas pressure. Additional physical insight is

provided by a *qualitative* comparison with the recent analysis of Gorlicke, Berman, and Khitrova[13] where they have considered the effects on the FWM spectrum of both velocity-changing collisions and the residual Doppler width (the result of the nonvanishing angle between the forward pump and probe beam.) For comparison with our experiments, we have also included the effects of collision-induced decay of the excitation due to loss of population, alignment, and orientation.

The cross-polarized experiment (the probe field is cross polarized with respect to the copolarized pump fields) shows that in a collisionless system, the NDFWM spectrum is characterized by a narrow dip due to nonconservation of alignment and orientation. However, at a few Torr of buffer gas, the dip has evolved into a spike due to "opening" of the system caused by state-changing and velocity-changing collisions. The fundamental width of both of the narrow features is determined by the inverse transit time, but is further broadened by the residual Doppler width. However, at higher pressures, velocity-changing collisions cause additional reduction in the width of the narrow spike, the amount of observed narrowing being limited by interlaser jitter. This narrowing is a form of Dicke narrowing. Finally, we illustrate the experimental results at different helium buffer gas pressure for copolarized experiments (all beams polarized in the same direction).

II. REVIEW OF THE THEORY

The measurements of collision-induced narrow resonances described in this paper are based on backward NDFWM as schematically represented in Fig. 1. Three incident waves $\mathbf{E}_p(\omega+\delta)$, $\mathbf{E}_f(\omega)$, and $\mathbf{E}_b(\omega)$ interact inside a sample, and a *coherent* signal wave $\mathbf{E}_s(\omega-\delta)$ is generated due to the induced third-order nonlinear optical polarization. Specifically, the signal wave is produced by the coherent scattering of the backward pump beam off an excitation grating which is a spatial and temporal modulation of population in a simple two-level system, or also of orientation and alignment if magnetic degeneracies are present. This spatial and temporal modulation is due to the interaction of the forward pump and probe beams inside the sample.

We begin by examining the theoretical results of a perturbation calculation of the NDFWM response using the quantum transport equation for the density-matrix operator and a strong collision model which is used to describe the interaction with ground-state perturbers. A simple two-level system is assumed as shown in Fig. 1. The theoretical work for a simple closed two-level system has been done by Gorlicki *et al.*[13] For completeness, we briefly discuss the details of the calculation. The results have been rederived to include the simple modification of adding the effects of collision-induced decay of the excitation (see second citation in Ref. 9.) However, the calculation reviewed here can only provide qualitative understanding of the physics since the presence of magnetic substates is not explicitly included. (For example, magnetic degeneracies give rise to alignment and orientation which, as we have shown earlier,[12] have an important effect on line shape in the absence of collisions.) Nevertheless, if we take levels 1 and 2 in Fig. 1 to represent the lower state and upper state of an excitation (such as population, alignment or orientation), then the calculations discussed in this section provide excellent insight into most of the physical behavior observed in the experiments. However, it is interesting to note that the current analysis is unable to account for the differences in line shape observed for different polarization configurations. These results are briefly discussed at the end of the paper.

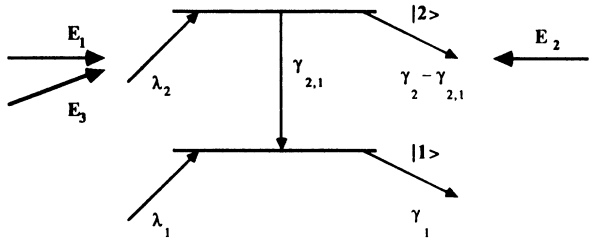

FIG. 1. Simple two-level system; level 2 decays to level 1 spontaneously at rate γ_{sp} and to the reservoir at rate $\gamma_2-\gamma_{sp}$; level 1 decays to the reservoir at rate γ_1.

The calculations are based on a solution of the equation of motion for the population density-matrix operator.[14] Assuming the strong collision model, the effect of velocity-changing collisions on the probabilities of being in levels 1 or 2 (the diagonal elements ρ_{ii} of the density matrix operator $\hat{\rho}$) is to give an extra decay rate Γ_i, and a source term due to atoms being scattered *into* resonance from different velocity subgroups. State-changing collisions (including magnetic sublevel-changing collisions) are incorporated as an additional loss rate, Γ_{sc}, on the upper level, ρ_{22}. (State-changing collisions are not considered as a source term for ρ_{22}.) On coherence (off-diagonal elements of ρ), the collisions produce a simple phase interruption resulting in pressure broadening. Mathematically, the collision terms are written as follows:

$$\left.\frac{\partial\rho_{22}(\mathbf{v},t)}{\partial t}\right|_{\text{col}} = -(\Gamma_2+\Gamma_{sc})\rho_{22}(\mathbf{v},t) + \int f_2(\mathbf{v}'-\mathbf{v})\rho_{22}(\mathbf{v}',t)d\mathbf{v}' , \tag{1}$$

$$\left.\frac{\partial\rho_{11}(\mathbf{v},t)}{\partial t}\right|_{\text{col}} = -\Gamma_1\rho_{11}(\mathbf{v},t)+\int f_1(\mathbf{v}'-\mathbf{v})\rho_{11}(\mathbf{v}',t)d\mathbf{v}' , \tag{2}$$

$$\left.\frac{\partial\rho_{12}(\mathbf{v},t)}{\partial t}\right|_{\text{col}} = -\Gamma_{12}\rho_{12}(\mathbf{v},t) . \tag{3}$$

In this model Γ_i and Γ_{ij} are independent of $\mathbf{v}$, and the kernel functions $f_i(\mathbf{v}'-\mathbf{v})$ are simply $w_0(\mathbf{v})\Gamma_i$, where $w_0(\mathbf{v})$ is the Maxwellian velocity distribution function. This means that, on average, the collisions thermalize the velocity distribution of the atom, regardless of the initial velocity of the atom.

For the two-level system, the equation of motion for the density-matrix elements including Doppler motion, velocity-changing, and state-changing collisions are

$$\left[\frac{\partial}{\partial t}+\mathbf{v}\cdot\nabla\right]\rho_{11}(\mathbf{v},t)$$
$$=-\tilde{\gamma}_1\rho_{11}(\mathbf{v},t)+\gamma_{sp}\rho_{22}(\mathbf{v},t)$$
$$-\frac{1}{i\hbar}[V_{21}\rho_{12}(\mathbf{v},t)-\rho_{21}V_{12}(\mathbf{v},t)]$$
$$+\Gamma_1 w_0(\mathbf{v})\int\rho_{11}(\mathbf{v}',t)dv'+\lambda_1\ , \tag{4}$$

$$\left[\frac{\partial}{\partial t}+\mathbf{v}\cdot\nabla\right]\rho_{22}(\mathbf{v},t)$$
$$=-\tilde{\gamma}_2\rho_{22}(\mathbf{v},t)+\frac{1}{i\hbar}[V_{21}\rho_{12}(\mathbf{v},t)-\rho_{21}V_{12}(\mathbf{v},t)]$$
$$+\Gamma_2 w_0(\mathbf{v})\int\rho_{22}(\mathbf{v}',t)dv'+\lambda_2\ , \tag{5}$$

$$\left[\frac{\partial}{\partial t}+\mathbf{v}\cdot\nabla\right]\rho_{12}(\mathbf{v},t)$$
$$=(i\omega_0-\tilde{\gamma}_{12})\rho_{12}(\mathbf{v},t)+\frac{1}{i}V_{12}[\rho_{22}(\mathbf{v},t)-\rho_{11}(\mathbf{v},t)]\ , \tag{6}$$

where the $\mathbf{v}\cdot\nabla$ term accounts for motion, $\mathbf{v}$ is the classical velocity associated with the center of mass, and V_{12} is the interaction potential between the dipole of the sample material and the incident classical electromagnetic fields of the form $-\boldsymbol{\mu}\cdot\mathbf{E}$.

$$\mathbf{E}=\tfrac{1}{2}\sum\mathbf{E}_m e^{i\mathbf{k}_m\cdot\mathbf{x}-i\omega_m t}+\text{c.c.}$$

is summed over all electromagnetic fields and μ is dipole moment operator (since this is a two-level model, we make the scaler approximation and ignore the vector nature of the interaction). Also $\tilde{\gamma}_1=\gamma_1+\Gamma_1$, $\tilde{\gamma}_2=\gamma_2+\Gamma_2+\Gamma_{sc}$, $\tilde{\gamma}_{12}=(\gamma_1+\gamma_2)/2+\Gamma_{12}$. Referring to Fig. 1 and in the absence of collisions, we see γ_1 is the lower-level decay rate which equals the transit rate γ_t if state 1 is the ground state; γ_2 is the excited-state decay rate which, in the absence of radiative decay to other levels, is given by $\gamma_{sp}+\gamma_t$; and γ_{sp} is the spontaneous emission rate to the lower level. Γ_1 and Γ_2 are the effective velocity-changing collision rates for state 1 and 2; Γ_{sc} is the state-changing collision rate for state 2. Γ_{12} is the extra dephasing rate due to all collisions. λ_1 and λ_2 are the velocity-dependent incoherent pumping rates which, along with the decay rates, establish the equilibrium value of the populations in the absence of optical excitation.[15]

If the nonlinear interaction is weak enough (i.e., we can ignore the coupled-mode problem), then the signal field is proportional to the nonlinear polarization P given by the integral over velocity of the $\mathrm{Tr}(\mu\rho)$. For weak incident fields, we use perturbation theory to solve the density-matrix equation to the third order in the applied electric fields. The result is

$$\rho_{12}^{(3)}(\mathbf{v},t)=\frac{-i\chi_b^*\chi_f^*\chi_p w_0(\mathbf{v})N_0\exp[i(\omega-\delta)t+i\mathbf{k}_p\cdot\mathbf{r}]}{8[i(\Delta-\delta)+i\mathbf{k}_p\cdot\mathbf{r}+\tilde{\gamma}_{12}]}$$
$$\times\left\{\left[\frac{1-R}{-i\delta+i\Delta\mathbf{k}\cdot\mathbf{v}+\tilde{\gamma}_1}+\frac{1+R}{-i\delta+i\Delta\mathbf{k}\cdot\mathbf{v}+\tilde{\gamma}_2}\right]\left[\frac{1}{i\Delta-i\mathbf{k}_f\cdot\mathbf{v}+\tilde{\gamma}_{12}}+\frac{1}{-i(\delta+\Delta)+i\mathbf{k}_p\cdot\mathbf{v}+\tilde{\gamma}_{12}}\right]\right.$$
$$\left.+(Z_{-\Delta}+Z_{\delta+\Delta})\left[\frac{(1-R)Z_1J_1}{-i\delta+i\Delta\mathbf{k}\cdot\mathbf{v}+\tilde{\gamma}_1}+\frac{(1+R)Z_2J_2}{-i\delta+i\Delta\mathbf{k}\cdot\mathbf{v}+\tilde{\gamma}_2}+\frac{RZ_2J_1J_2}{-i\delta+i\Delta\mathbf{k}\cdot\mathbf{v}+\tilde{\gamma}_1}\left[\frac{1}{\Gamma_2}-\frac{1}{\Gamma_1}\right]\right]\right\}$$
$$+(\text{terms with }\mathbf{k}_f\rightarrow-\mathbf{k}_f)\ , \tag{7}$$

where $N_0=\rho_{11}^{(0)}-\rho_{22}^{(0)}$ is the population difference in the absence of fields, $\Delta=\omega_f-\omega_0$, $\delta=\omega_p-\omega_f$, $\Delta\mathbf{k}=\mathbf{k}_p-\mathbf{k}_f$, where ω_i and $\mathbf{k}_i$ $(i=f,p)$ are the frequency and wave vector of the forward pump and probe beam, respectively, and ω_0 is the atomic resonant frequency. Also $\chi_m=\mu_{12}E_m/\hbar$ is the Rabi frequency $(m=p,f,b)$, $R=\gamma_{sp}/(\tilde{\gamma}_2-\tilde{\gamma}_1)$. In addition,

$$J_i=\Gamma_i\left[1-\Gamma_i\int d\mathbf{v}w_0(\mathbf{v})/(-i\delta+i\Delta\mathbf{k}\cdot\mathbf{v}+\tilde{\gamma}_i)\right]^{-1}=\Gamma_i(1+i\Gamma_i Z_i/\Delta ku)^{-1}\ ,$$

where $i=1,2$. For i, $Z_i=Z(\xi_i)$ and $\xi_i=(\delta+i\tilde{\gamma}_i)/\Delta ku$; for $\alpha=-\Delta$, $\delta+\Delta$, or $\delta-\Delta$, $Z_\alpha=Z[(\alpha+i\tilde{\gamma}_{12})/ku]$. Z is the plasma dispersion function defined as

$$Z(\zeta)=(\sqrt{\pi})^{-1}\int_{-\infty}^{+\infty}dx\ \exp(-x^2)/(x-\zeta)$$

for $\mathrm{Im}\zeta>0$. Physically, ku represents the Doppler width and Δku ($\Delta k=|\Delta\mathbf{k}|$) represent the residual Doppler width due to the nonvanishing angle between the forward pump and probe beam. The terms given by $(\mathbf{k}_f\rightarrow-\mathbf{k}_f)$ represent signal from the forward pump scattering off the excitation grating formed by the backward pump and the probe beam, which is much smaller (due to thermal motion[16]) than the signal from the backward pump scattering off the grating formed by the forward pump and the probe beam.

The nonlinear polarization is the average of $\mu_{21}\rho_{12}$ + c.c. over velocity for the atomic system. This is carried out in the Doppler limit: $|\Delta|,\delta,\tilde{\gamma}_{12},\tilde{\gamma}_i\ll ku$; and in the small angle limit $\varphi\ll1$ (φ is the angle between the forward pump and the probe). In this case, we can set $|\mathbf{k}_p|\cong|\mathbf{k}_f|=k$; $\mathbf{k}_f\cdot\mathbf{v}=kv_z$; $\mathbf{k}_p\cdot\mathbf{v}=kv_z+\Delta kv_y$; $(\mathbf{k}_p-\mathbf{k}_f)\cdot\mathbf{v}=\Delta kv_y$, where $\Delta k\cong k\varphi$. Finally, the integration over v_z and v_y can be performed analytically to give the polarization

$$P^{\mathrm{NL}}(t)=-\tfrac{1}{8}i\mu_{21}\chi_b^*\chi_f^*\chi_p N_0\exp[i(\omega-\delta)t+i\mathbf{k}_p\cdot\mathbf{r}]$$
$$\times\left\{\frac{Z_{\delta-\Delta}+Z_{-\Delta}}{-iku(\Delta ku)^2}\left[(1-R)\frac{Z_{12}-Z_1}{\xi_{12}-\xi_1}+(1+R)\frac{Z_{12}-Z_2}{\xi_{12}-\xi_2}\right]+\frac{Z_{\delta+\Delta}-Z_{\delta-\Delta}}{(-2i\Delta)ku(\Delta ku)}[(1-R)Z_1+(1+R)Z_2]\right.$$
$$\left.+\frac{Z_{\delta-\Delta}(Z_{\delta+\Delta}+Z_{-\Delta})}{(ku)^2(\Delta ku)^2}\left[(1+R)J_2Z_2^2+(1-R)J_1Z_1^2+RJ_1J_2Z_1Z_2\left[\frac{1}{\Gamma_2}-\frac{1}{\Gamma_1}\right]\right]\right\}+\text{c.c.}\,, \tag{8}$$

where $Z_{12}=Z(\xi_{12})$ and $\xi_{12}=(\delta-2\Delta+2i\bar{\gamma}_{12})/\Delta ku$. After integration, we have neglected those terms which are smaller by a factor of $\bar{\gamma}_{12}/ku$ (including those terms of the form $\mathbf{k}_f\rightarrow-\mathbf{k}_f$).

III. EXPERIMENTAL CONFIGURATION

Figure 2 illustrates the experimental configuration. An argon ion laser pumps two frequency-stabilized single-mode cw dye lasers (Coherent model 699-21) with a peak-to-peak inter-laser jitter of order 3 MHz. The beam from the first dye laser is used to provide the counterpropagating pump beams at frequency ω. The beam from the second dye laser is used to provide the probe beam at frequency $(\omega+\delta)$. Because of phase-matching conditions, the signal beam at frequency $(\omega-\delta)$ is counterpropagating with respect to the probe beam and is directed to a photomultiplier tube (PMT) by a beam splitter.

The laser providing the pump beams is tuned to the high-frequency side of the Na transitions $3s\,^2S_{1/2}(F=2)-3p\,^2P_{3/2}(F=3)$ to minimize contributions from the nearby hyperfine levels. To reduce the residual Doppler width, the two counterpropagating pump beams are aligned interferometrically to be exactly counterpropagating, while the angle between the forward pump and probe is adjusted to be less than 2 mrad (measured in the plane of incidence) and less than 0.4 mrad (measured out of the plane of incidence). The small angle is required in order to permit us to carefully examine the evolution of the spectral response on the presence of state-specific collisions. In earlier work,[10] the residual Doppler width dominated the measurements. However, at this reduced angle, as we see below, it is even possible to see the effects of radiative-decay-induced narrow resonances due to nonconservation of alignment and orientation.[12] The spectral response is measured as a function of the probe frequency.

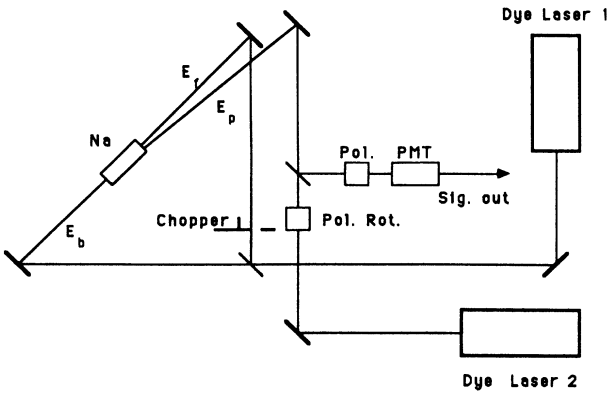

FIG. 2. Experimental configuration in NDFWM.

A chopper is used to modulate the forward pump beam to enable phase-sensitive detection. The Data 6000 (Data Precision) system is used for averaging the signal from a lock-in amplifier. The sodium density is of the order $1\times10^{10}/\mathrm{cm}^3$ in a 10-cm cell. The buffer gas is helium and the buffer gas pressure is measured with a Baratron gauge. Helium was used to minimize the effect of collision-induced optical pumping[9] which reduces the signal to noise. (Helium is clearly not well described by the strong collision model, and hence the velocity-changing collision rates used in comparison with experiment must be considered to be effective collision rates.)

IV. DISCUSSION OF RESULTS

In this section we discuss the dependence of the NDFWM line shape on buffer-gas pressure.

Physical insight into the understanding of NDFWM can be gained by considering the simple two-level system shown in Fig. 1. In the absence of collisions, the analysis provided above simplifies considerably[17,18] (see also discussion of physics of two-level systems in Ref. 19). In Fig. 1 γ_1 is the decay rate out of the state one. γ_2 is the total decay rate out of state two which consists of γ_{sp}, the spontaneous emission rate from state two to state one, and $\gamma_2-\gamma_{\mathrm{sp}}$, the decay rate from state two to the reservoir. Generally, in backward NDFWM spectroscopy studies of an inhomogeneously broadened atomic two-level system, the pump frequency is fixed at $\omega=\omega_0+\Delta$ ($\Delta\ll ku$ for near-resonance detuning). Two resonances are observed as a function of pump-probe detuning δ; one is at $\delta=0$ and the other is at $\delta=2\Delta$. The $\delta=0$ resonance is associated with the dynamics of the ground state and the excited state and is the sum of two resonances resulting from a coupled interaction between the forward pump and the probe beam. The widths of the two resonances are $2\gamma_1$ and $2\gamma_2$, respectively. The second resonance ($\delta=2\Delta$) reflects contributions to the nonlinear response from both a one-photon process (absorption) and a three-photon process (absorption of two pump photons and emission of a probe photon). The width of this resonance is determined by the dephasing rate of the induced optical dipole and is given by $4\bar{\gamma}_{12}$. The focus of this paper is on the $\delta=0$ structure.

We define a closed two-level system by the condition. $\gamma_2=\gamma_{\mathrm{sp}}+\gamma_1$. For the case that state 1 is the ground state, γ_1^{-1} is the transit time, and we see that a closed system is one that conserves population (to within an overall decay constant due to transit-time effects). For a simple

closed two-level system, it is easy to show that the amplitude of the $\delta=0$ resonance having width $2\gamma_1$ is zero.[18] Hence, the $\delta=0$ resonance is characterized by a width $2\gamma_2$. However, in an open two-level system (where the total population is not conserved), a narrow resonance with width given by the lower-state decay rate is observed. If $\gamma_2-\gamma_{sp}>\gamma_1$, a narrow peak appears; however, for certain values of γ_2 and γ_1 if $\gamma_2-\gamma_{sp}<\gamma_1$, a narrow resonance of width $2\gamma_1$ contributes negatively resulting in a dip.[18] In the latter case, the linewidth of both narrow features is limited by the residual Doppler width $ku\varphi$ and the laser jitter (if $\gamma_1 \ll ku\varphi$ and the laser jitter).

As discussed earlier, an open system can result from a decay out of the excited state to a state other than the lower state of the transition (for example, due to optical pumping). It could also be induced by state-changing and velocity-changing collisions. In the case of velocity-changing collisions with different collision rates for states 1 and 2, even though the total population may be conserved, the collisions can cause a decay of the population in the specific laser selected velocity subclass. Thus, the velocity subgroup population which resonantly interacts with incident fields is no longer conserved. Therefore, velocity-changing collisions can directly lead to the appearance of the resonance having width γ_1.

However, in a two-level system characterized by magnetic substate degeneracy, even though the population is conserved, the orientation and alignment need not be conserved. Since orientation and alignment contribute to the signal, nonconservation of orientation or alignment also results in a narrow feature characterized by the lower-state decay rate.[12] This feature can contribute positively or negatively resulting in a spike or dip in the $\delta=0$ resonant structure.

Therefore, in general, in a four-wave-mixing spectroscopy study of a resonant transition, narrow features in the spectrum appear whenever there exists a nonconservation of population, orientation, or alignment because of coupling to the reservoir (including radiative decay). Moreover, these general concepts can be extended to systems characterized by symmetry other than spherical symmetry such as found in solids.

The essential features of the above discussion are seen in the spectra shown in Fig. 3 obtained using the experimental configuration discussed above. In Fig. 3 the pump beams are vertically polarized and the probe beam is cross polarized with respect to the pumps. The signal is polarized parallel to the probe beam.[20] Using cross-polarized light reduces the significance of contributions from the nearby hyperfine levels.[12] In this case, the spatial and temporal modulation of the upper- and lower-level excitation is associated with alignment and orientation, rather than pure populations. Thus, as indicated earlier, comparison with a two-level theory must be considered qualitatively where the populations in states 1 and 2 of the theory represent general lower- and upper-level excitations. Collisional effects then cause a decay of these excitations.

The NDFWM response with a 0-Torr buffer gas is shown in Fig. 3(a) and is similar to that reported elsewhere.[12] As mentioned earlier, the first resonance at $\delta=0$ is striking because of the presence of a narrow resonance. In the absence of collisions, this transition is closed with respect to population, but alignment and orientation are not conserved (i.e., the system is open with respect to alignment and orientation due to optical pumping). The nonconservation of alignment and orientation leads to the contribution at $\delta=0$ from the resonance with a width characterized by the ground-state decay rate $\gamma_1(\gamma_1=\gamma_t\cong 0.1$ MHz). The contribution is negative, resulting in a dip which is broadened by the residual Doppler width ($\cong 2$ MHz) due to the finite angle between the probe and the forward pump beam and by the interlaser jitter.

Since the model leading to Eq. (8) does not include magnetic substate degeneracy, we can not expect to predict the exact structure in Fig. 3(a). However, the narrow dip can be interpreted as a residual long-lived perturbation of the ground state (due to optical pumping) which can be seen in a simple two-level model if $\gamma_2-\gamma_{sp}<\gamma_1$. The spectral response predicted in Eq. (8) at a pressure of 0 Torr is shown in Fig. 3(e) with $\gamma_1=0.1$, $\gamma_2-\gamma_{sp}=0.01$, $\varphi=0.0019$ rad (all decay rates and frequencies are normalized to $\gamma_{sp}=10$ MHz). For comparison with the remaining experiments, these values ($\gamma_1,\gamma_2-\gamma_{sp},\varphi$) are kept constant in the following theoretical plots.

At a pressure of 5.8 Torr in Fig. 3(b), a spike on top of a wide peak is observed at the $\delta=0$ resonance, which is due to the fact that buffer-gas collisions result in an open system due to the effects of state-changing (including magnetic substate changing) and velocity-changing collisions. The dip in Fig. 3(a) has evolved into a spike because the effect of collision-induced decay exceeds the effect of optical pumping (i.e. $\gamma_2-\gamma_{sp}+\Gamma_{sc}>\gamma_1$) thus leading to a positive contribution from the narrow lower-level resonance. The spike has a width $2\gamma_1$ which is due to the contribution from the ground state, but it is further broadened by the residual Doppler width $ku\varphi$. The wide peak has a width $2(\gamma_2+\Gamma_{sc})$ which is due to the contribution from the excited state. The $\delta=2\Delta$ resonance representing the coherence between states 1 and 2 is pressure broadened as seen in the Fig. 3(b). The corresponding theory is plotted in Fig. 3(f) with $\Gamma_{sc}/\Gamma_2=0.5$, $\Gamma_1/\Gamma_2=0.73$, $\Gamma_{12}/\Gamma_2=3.2$, and $\Gamma_2=1.9$ MHz/Torr. Again Γ_1 and Γ_2 are the effective velocity-changing collisions rates for states 1 and 2, Γ_{sc} is the state change collision rate (including magnetic sublevel changing collisions) and Γ_{12} is the extra dephasing rate due to all collisions.

Figure 3(c) shows the experimental result at a pressure of 10 Torr. A very narrow spike sitting on a pedestal is observed and the line width of the spike is now *below the residual Doppler width.* This is because at high pressure, collisions reduce the mean free path of the active atoms to the point that it is less than the grating spacing produced by the spatial modulation of the forward pump and probe. Thus in the limit $u/\Gamma_1 \ll (|\Delta k|^{-1})$ residual Doppler broadening does not contribute to the narrow spike, and the linewidth is limited by inter-laser jitter. This line shape is closely related to Dicke narrowing of radiative transitions even though the narrowing occurs on modulated atomic-state excitations. The broad pede-

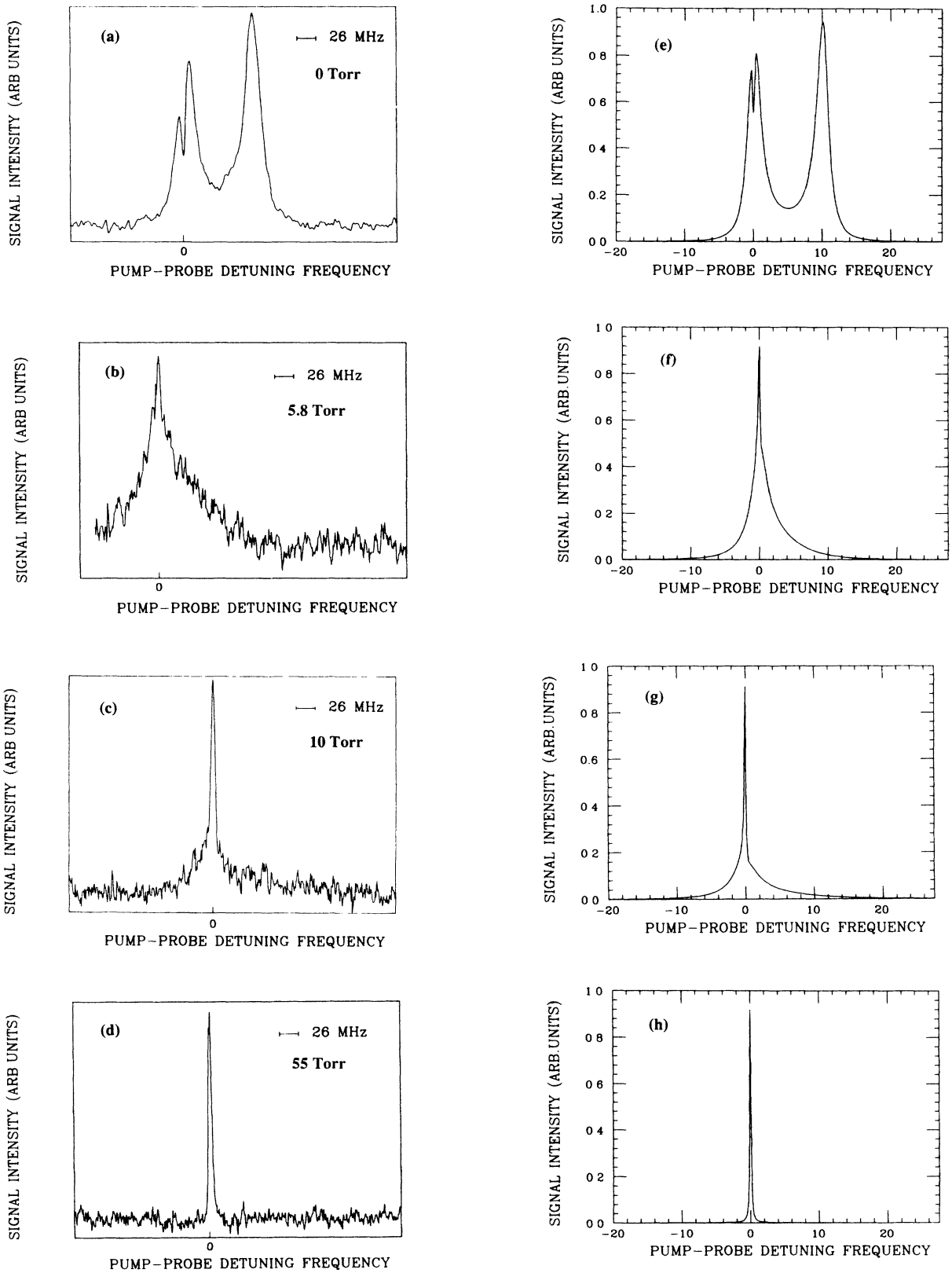

FIG. 3. (a)–(d) are the NDFWM spectrum of the Na transition $3s\,^2S_{1/2}(F=2)\rightarrow 3p\,^2P_{3/2}(F=3)$ at different He pressure P. All beams are linearly polarized and the probe beam is cross polarized relative to the pump beams. In (a), (c), and (d) $\Delta/2\pi=51$ MHz; in (b) $\Delta/2\pi=30$ MHz. (a) $P=0$ Torr, (b) $P=5.8$ Torr, (c) $P=10$ Torr, (d) $P=55$ Torr. (e)–(h) are corresponding theoretic plots with $\varphi=0.0019$ (rad), $\gamma_1=0.1$, $\gamma_2=1.01$, $\gamma_{sp}=1$ (all γ's and detuning frequency are normalized to $\gamma_{sp}=10$ MHz), $\Gamma_1/\Gamma_2=0.73$, $\Gamma_{sc}/\Gamma_2=0.5$, $\Gamma_{12}/\Gamma_2=3.2$.

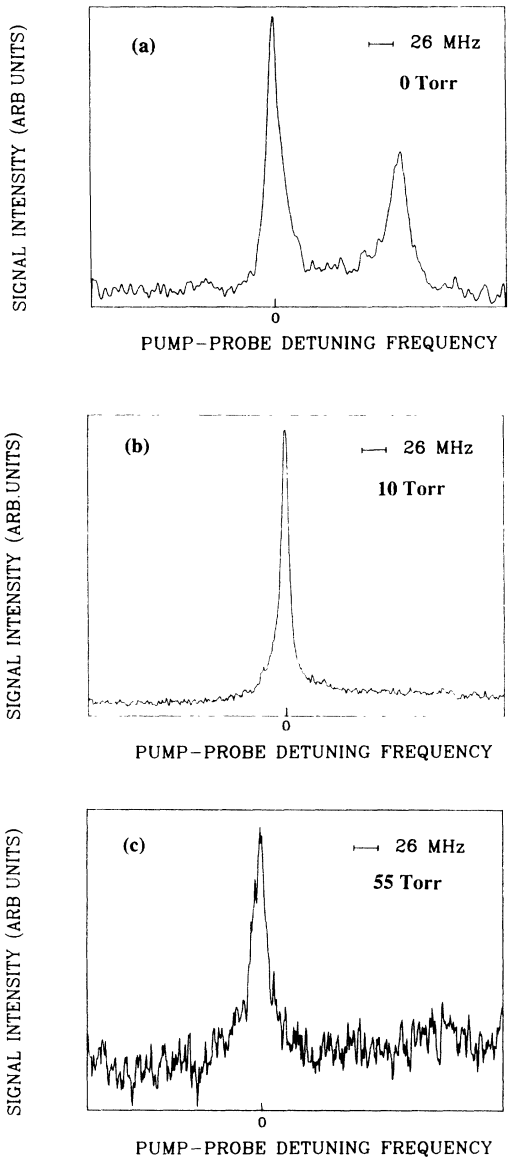

FIG. 4. The experimental NDFWM spectrum of Na transition $3s\ ^2S_{1/2}(F=2) \rightarrow 3p\ ^2P_{3/2}(F=3)$ at different He pressure P. All beams are linearly polarized in the same direction. (a) $P=0$ Torr, (b) $P=10$ Torr, (c) $P=55$ Torr, $\Delta/2\pi=73$ MHz.

stal is again due to the contribution from the excited state with width $2(\gamma_2+\Gamma_{sc})$. Figure 3(g) shows the corresponding plot of the theory at this pressure.

Figure 3(d) shows the experimental result at a pressure of 55 Torr. At such higher pressure ($\Gamma_i/\gamma_i > ku/\bar{\gamma}_{12}$), we would expect that the system "recloses" and the $\delta=0$ resonance approaches its homogeneous linewidth $2\gamma_2$ (see Ref. 13 for a detailed discussion). But because of the state-changing collisions, the system remains open. Therefore, a width $2\gamma_1$ of the $\delta=0$ resonance is expected which is limited by the laser jitter due to the Dicke narrowing. The excited-state contribution with width $2(\gamma_2+\Gamma_{sc})$ is totally suppressed because the intensity of the resonance is inversely proportional to the square of the width. Figure 3(h) shows the corresponding theoretical result.

As indicated earlier, the NDFWM profiles shown in Fig. 3 were obtained using orthogonally polarized pump and probe beams. It was shown in Ref. 12 that under these conditions, the contribution from nearby resonances was minimal. This was not the case for the copolarized pump and probe experiments. In this case, the theory, which included only the $F=2$ to $F=3$ transition, predicted a dip in the NDFWM spectra (similar to the cross-polarized experiments), while the experiments showed a spike. Agreement between theory and experiment was obtained when contributions from the nearby resonances were included in the theory.

Even though there appear to be the above-mentioned additional complications associated with the copolarized experiments, it is instructive to examine the evolution of the copolarized NDFWM spectra as a function of buffer-gas pressure. Figure 4 shows the copolarized data obtained at three different buffer-gas pressures of 0, 10, and 55 Torr. The results are significantly different from those of Fig. 3. In addition, given the experimental parameters, there is no real agreement between theory and experiment. Most profound is the difference between the simple analysis and the experiment at high pressure (55 Torr). The experiment shows a NDFWM profile which would be expected if the system was closed. Indeed, if the state-changing collision rate is set to zero, the analysis provides a NDFWM profile similar to the observed result. However, clearly, state-changing collisions guarantee that the system is open. Our current work is addressing a more complete description of collision effects.

In conclusion, we have shown that when the system experiences velocity-changing and state-changing collisions, the line shape of the $\delta=0$ resonance evolves from a dip at $p=0$ Torr to a narrow spike with a width below residual Doppler width at $p=55$ Torr in the cross-polarized experiment. Velocity-changing collisions redistribute the atoms among different velocity subgroups and induce a decay of the resonant-selected-velocity subgroup to other velocity subgroups. State-changing collisions contribute to the decay of the excitation in the upper level. Both of these effects lead to the appearance of a narrow resonance with a width below that given by the spontaneous emission rate.

ACKNOWLEDGMENTS

The authors wish to acknowledge helpful discussions with Professor Paul Berman. This work is supported by the U.S. Army research office (Grant No. DAAL-03-86-K-0057).

[1]N. Bloembergen, H. Loten, and R. T. Lynch, Jr., Indian J. Pure and Appl. Phys. **16**, 151 (1978); N. Bloembergen, in *Laser Spectroscopy IV,* edited by H. Walther and K. W. Rotha (Springer, Berlin, 1979), pp. 340–348.

[2]Y. Prior, A. R. Bogdan, M. Dagenais, and N. Bloembergen, Phys. Rev. Lett. **46**, 111 (1981).

[3]G. Grynberg, J. Phys. B **14**, 2089 (1981).

[4]H. Friedmann and A. D. Wilson-Gordon, Phys. Rev. A **26**, 2768 (1982).

[5]H. Friedmann and A. D. Wilson-Gordon, Phys. Rev. A **28**, 302 (1983); A. D. Wilson-Gordon and H. Friedmann, *ibid.* **30**, 1377 (1984).

[6]Y. Prior, I. Schek, and J. Jortner, Phys. Rev. A **31**, 3775 (1985).

[7]L. Rothberg, in *Progress in Optics,* edited by E. Wolf (Elsevier, Amsterdam, 1987), pp. 39–101.

[8]R. K. Raj, D. Bloch, J. J. Snyder, G. Camy, and M. Ducloy, Phys. Rev. Lett. **44**, 1251 (1980).

[9]D. G. Steel and R. A. McFarlane, Phys. Rev. A **27**, 1217 (1983); **27**, 1687 (1983).

[10]J. F. Lam, D. G. Steel, and R. A. McFarlane, Phys. Rev. Lett. **49**, 1628 (1982); **56**, 1679 (1986).

[11]Jing Liu, J. T. Remillard, and D. G. Steel, Phys. Rev. Lett. **59**, 799 (1987).

[12]P. R. Berman, D. G. Steel, G. Khitrova, and J. Liu, Phys. Rev. A **38**, 252 (1988).

[13]M. Gorlicki, P. R. Berman, and G. Khitrova, Phys. Rev. A **37**, 4340 (1988).

[14]See for instance, P. R. Berman, in *New Trends in Atomic Physics,* Proceedings of the Les Houches Summer School of Theoretical Physics, Session 38, 1982, edited by G. Grynberg and R. Stora (North-Holland, Amsterdam, 1984), p. 451; P. R. Berman, Phys. Rev. A **5**, 927 (1972).

[15]Willis E. Lamb, Phys. Rev. **134**, A1429 (1964).

[16]J. F. Lam and R. L. Abrams, Phys. Rev. A **26**, 147 (1982).

[17]A. D. Wilson-Gordon and H. Friedmann, Opt. Lett. **8**, 617 (1983). (This paper describes the ground-state decay as originating from collisions. However, since no collisional redistribution term is included, the decay they discuss is not limited to collisions. In addition though, without this redistribution term, the sub-Doppler narrowing effects will not be predicted by their analysis.)

[18]D. G. Steel and J. T. Remillard, Phys. Rev. A **36**, 4330 (1987).

[19]Galina Khitrova, Paul R. Berman, and Murray Sargent III, J. Opt. Soc. Am. B **5**, 160 (1988).

[20]J. F. Lam, D. G. Steel, R. A. McFarlane, and R. C. Lind, Appl. Phys. Lett. **38**, 977 (1981).